MODELING OF AVOIDING WINDOW-TYPE HEAT PUMP FROST THROUGH HEAT RECOVERY SYSTEM

Di Liu, Mrs., College of Civil Engineering, Hunan University, Changsha, China
Guangfa Tang, Professor, College of Civil Engineering, Hunan University, Changsha, China
Fuyun Zhao, PhD., College of Civil Engineering, Hunan University, Changsha, China

ABSTRACT

An ideal mathematic model is developed for widow-type air-conditioner evaporator with heat recovery system under frosting condition. The exhaust hot indoor air passing through the heat recovery system would be fed to the evaporator, which could increase the total air source mixture temperature, and mixed air characteristics would be calculated through mass and energy conservation. A parametric analysis is performed to investigate the effects of air inlet temperature, relative humidity and air mass flow rate on total heat transfer coefficient, frost thickness and airside pressure drop separately. That rationalizing ratio and characteristics of indoor air and outdoor air could prolong frosting time and reduce the frost thickness greatly. Total heat transfer, frost thickness and airside pressure drop will increase with the time diminishes. They increase non-linearly with frosting time, fast increase at the start and gradually slowing down afterwards. A higher air mass flow rate would result in less frost accumulation. However, this could increase the resistance to airflow, and the airside pressure drop.

Key Words: ***modeling, avoiding frost, window-type heat pump, heat recovery system.***

1 INTRODUCTION

Room air-conditioner is well used nowadays, compared to some years ago. However, when such a unit operates as a heating source under low ambient temperature in winter, the formation of frost on the surface of its airside heat exchanger becomes problematic, leading to the degradation of the heat exchanger's performance. These result in the lower heat transfer efficiency, a higher airside pressure drop and reducing the heating capacity. In this time, defrosting should be carried out. The traditional defrosting method is reverse cycle of the refrigerant through four-direction valve from the heating mode to the cooling mode, and then the part of indoor heat, the power of compressor, and the heat stored in the indoor heat exchanger and the condenser should be used to defrost, which lead to the discomfort of residents. The formation of frost may sometimes even cause the shutdown of a unit. Jones and Parker (1975), Miller (1978), Marinyuk (1980), Young (1980), Sami and Duong (1989), and O'Neal et al. (1989) have investigated the frost and defrost properties. Jones and Parker (1975) studied frost formation on flat plates and found that increase of relative humidity of ambient air increased the frost formation rate, but increase of air velocity decreased the frost formation rate. Sami and Duong (1989) developed a model to calculate the frost thickness and frost density for flat surfaces. Model results showed that increase of relative humidity or decrease of surface temperature accelerated frost formation. Yonko and Sepsy (1967) examined frost formation on flat plates and reported that the thermal conductivity of frost varied with its density. Liu et al. (2003) have studied simulation of air-source heat pump during hot-gas defrost. In their paper, a defrost model was presented and an experiment to validate the model was conducted.

Most of the studies mentioned above were based on investigation of frost properties and the heat transfer involved in the frost growth or defrost process to avoid frost or defrost. However, avoiding window-type heat pump frost through heat recovery system has been studied little among the amount of literature available. In this paper, an ideal frost model is presented based on the fundamental conservation equations and experimental results. The influence of the exhaust airflow is included. The distribution parameter method is adopted to study the details of the heat and mass transfer at the frost and defrost process. A finned-plate heat exchanger as a heat recovery facility is designed for air-conditioning exhaust system. A window-type heat pump is chosen to combine with the heat recovery facility. In the facility, the cold outdoor air absorbs the energy of exhaust air and energy saving is achieved. The exhausted hot indoor air passing through the heat recovery system would be fed to the evaporator, which could increase the total air source mixture temperature. In this way, the temperature of evaporating coils becomes higher, and could avoid the formation of the frost.

2 MODEL DESCRIPTION

This model has two parts: the one is frosting sub-model and the other is heat exchanger sub-model, in which there are three modules, i.e., refrigerant side, pipe wall side and air side. For simplicity, hypotheses have been made as follows:

1. Refrigerant in both liquid and gas phase is considered incompressible and in a thermal equilibrium.
2. Both kinetic energy and potential energy are neglected in energy conservation equation.
3. A linear relationship between saturated air enthalpy and air dry bulb temperature is assumed, with air temperature ranging from –25 to 30 °C, or $h_a=a+a_1t_a$
4. The heat transfer by radiation between the moist air and frost is negligible.
5. The density and thermal conductivity of each frost layer are entirely dependent on the interface temperature between air and frost.
6. Refrigerant flows in one-dimension along the heat exchanger pipe exist.
7. Problem is assumed to be quasi-steady-state.

2.1 The Frost Mass Accumulated upon the Evaporator Surface

The frost accumulation upon the evaporator surface is related to the absolute humidity difference between evaporator airflow inlet and outlet.

$$\dot{m}_{ft} = \dot{m}_a (d_i - d_o) \tag{1}$$

Consider the water vapor being transported to a surface during the process of frost formation. Part of this water vapor will be diffused into the exiting layer of frost before it freezes, which serves to increase the frost density. The rest of this water vapor freezes out at the frost surface, which serves to increase the frost thickness.

$$\dot{m}_{fr} = \frac{d}{dt}(\delta_{fr}\rho_{fr}) = \rho_{fr}\frac{d\delta_{fr}}{dt} + \delta_{fr}\frac{d\rho_{fr}}{dt} \tag{2}$$

$$\dot{m}_{\delta} = \rho_{fr}\frac{d\delta_{fr}}{dt}, \dot{m}_{\rho} = \delta_{fr}\frac{d\rho_{fr}}{dt} \tag{3}$$

$$\dot{m}_{fr} = \dot{m}_{\delta} + \dot{m}_{\rho}$$

(4)O'Neal et al. (1989) used the following expression for the amount of water vapor diffusing through a porous frost layer,

$$\dot{m}_{\rho} = A_t D_s \left[\frac{1-(\rho_f / \rho_i)}{1+(\rho_f / \rho_i)^{0.5}} \right] \frac{d\rho_v}{dx} \tag{5}$$

Using ideal gas state equation with unit mass ($p_v = \rho_v R T_s$), then

$$\frac{dp_v}{dx} = \frac{d}{dx}(\rho_v R T_s) = R\left[\frac{d}{dx}(\rho_v T_s) \right] = R\left[\rho_v \frac{dT_s}{dx} + T_s \frac{d\rho_v}{dx} \right] \tag{6}$$

This can be rewritten as:

$$\frac{d\rho_v}{dx} = \frac{1}{RT_s}\left(\frac{dp_v}{dT_s} - \frac{p_v}{T_s}\right)\frac{dT_s}{dx} \tag{7}$$

The Clapeyron-Clausius equation is

$$\frac{dp_v}{dx} = \frac{h_{sb}}{T_s(\nu_v - \nu_i)} \tag{8}$$

Substituting equations (7) and (8) into equation (5), the result is described by:

$$\dot{m}_{\rho} = A_t D_s \left[\frac{1-\left(\rho_f / \rho_i\right)}{1+\left(\rho_f / \rho_i\right)^{0.5}} \right] \left(\frac{1}{RT_s} \right) \left(\frac{h_{sb}}{T_s\left(\nu_v - \nu_i\right)} - \frac{p_v}{T_s} \right) \frac{dT_s}{dx} \tag{9}$$

Based on energy transportation, the total energy transferred to the frost layer includes sensible heat transferred from air and the latent heat of solidification released by water vapor as it diffuses into the frost layer and solidifies. That is given by,

$$\dot{Q}_t = A_t \lambda_{fr} \frac{dT_s}{dx} + \dot{m}_{\rho} h_{sb} \tag{10}$$

Substituting the equation (11) into the equation (10), the result is,

$$\dot{m}_{\rho} = \frac{\dot{Q}_t}{h_{sb} + \lambda_{fr} R T_s^{\,2} \Big/ \left\{ D_s \left[\frac{1-\left(\rho_{fr} / \rho_i\right)}{1+\left(\rho_{fr} / \rho_i\right)^{0.5}} \right] \left(\frac{h_{sb}}{\nu_v - \nu_i} - p_v \right) \right\}} \tag{11}$$

2.2 The Total Heat Transfer

2.2.1 The heat transfer on the air-frost interface

The sensible and latent heat transfer occurs simultaneously on the air-frost interface.

$$Q = c_a A_T \left(T_{ai} - T_{sur}\right) + c_m A_T h_{sv} (d_{ai} - d_{sur}) \tag{12}$$

The mass coefficient, c_m, is related to the heat transfer coefficient by the Lewis number.

$$c_m = \frac{c_a}{Le \cdot c_p} \tag{13}$$

If the latent heat term on the right-hand side of the Eq. (12) is written like the sensible heat transfer term, Eq. (14) is obtained.

$$Q = c_a A_T (T_{ai} - T_{sur}) + c_{lat} A_T (T_{ai} - T_{sur}) \tag{14}$$

where,

$$c_{lat} = \frac{c_a (d_{ai} - d_{sur}) h_{sv}}{Le \cdot c_p (T_{ai} - T_{sur})} \tag{15}$$

The total heat transfer, latent and sensible, can be expressed as,

$$Q = (c_a + c_{lat}) A_T (T_{ai} - T_{sur}) = c_{eff} A_T (T_{ai} - T_{sur}) \tag{16}$$

2.2.2 The heat transfer from moist air to the frost layer

The total heat transfer from moist air to the frost layer is the sum of heat conduction inside the frost layer (Q_{con}) and sublimation of the water vapor form the moist air (Q_{sub}).

$$Q = Q_{con} + Q_{sub} = A_T k_{fr} (\frac{dT}{dx})_s + \dot{m}_\rho h_{sv} \tag{17}$$

From the above assumptions, the heat transfer equation in a differential control volume is written as,

$$\frac{dQ_{con}}{dx} + \frac{dQ_{sub}}{dx} \approx 0 \tag{18}$$

By using Eq. (18), Eq. (17) can be reduced to Eq. (19).

$$k_{fr} A_T \frac{d}{dx}\left(\frac{dT}{dx}\right) = -h_{sv} \frac{d\dot{m}_\rho}{dx} \tag{19}$$

Since it has been assumed that the frost density does not vary with x, then the amount of water vapor being frozen must be the same everywhere in the frost layer. This results in,

$$\frac{d\dot{m}_\rho}{dx} = \frac{\dot{m}_\rho}{\delta_{fr}} \tag{20}$$

Combining the Eq. (19) and Eq. (20), we could obtain that,

$$\frac{d^2 T}{dx^2} = -\frac{h_{sv} \dot{m}_\rho}{k_{fr} A_T \delta_{fr}} \tag{21}$$

The boundary conditions of Eq. (21) can be given by,

T=T_p at x=0

$$\frac{dT}{dx} = \frac{Q - \dot{m}_\rho h_{sv}}{k_{fr} A_T} \quad \text{at} \quad x = \delta_{fr}$$

Integrating the Eq. (21), the temperature distribution could be expressed below,

$$T = -\frac{\dot{m}_\rho h_{sv}}{2A_T k_{fr}\delta_{fr}} x^2 + \frac{Q}{A_T k_{fr}} x + T_p \tag{22}$$

The following correlation is used to calculate the heat transfer coefficient(Karatas 1995).

$$c_a = 0.113\,\mathrm{Re}^{0.775}\,\mathrm{Pr}^{1/3}\,\varepsilon^{-0.420}\,\frac{k_a}{d_0} \tag{23}$$

Pierre's correlation that has been used by Hambraeus (1991) is chosen to calculate the refrigerant side heat transfer coefficient.

$$c_i = \frac{k_l}{d_i} 0.0082\left[\mathrm{Re}_{lo}^2\, k_f\right]^{0.4} \tag{24}$$

The evaporator of the Window-type used in this study has fin geometry. The fin efficiency is adopted from Kondepudi and O'Neal (1993).

$$\eta_f = \frac{th(m\cdot L)}{m\cdot L} \tag{25}$$

$$m = \sqrt{\frac{1}{c_{p\cdot a}/(\alpha_{a.s}\cdot a_1)+\delta_{fr}/\lambda_{fr}}\cdot\frac{1}{\lambda_f\delta_f}} \tag{26}$$

Where the fin equivalent height *L* is calculated by Kondepudi and O'Neal (1993),

$$L = \frac{D_0}{2}(\tau - 1)(1 + 0.35\ln\tau)$$

$$\tau = 1.063 S_1 / D_0$$

From Sanders (1974), the surface efficiency is defined as,

$$\eta_s = 1 - \frac{A_f}{A_T}\cdot(1-\eta_f) \tag{27}$$

The overall heat transfer coefficient of the evaporator can be calculated as,

$$UA_T = \left(\frac{1}{\eta_f\cdot c_{eff}\cdot A_T} + \frac{1}{c_i A_i} + \frac{\delta_f}{k_f\cdot A_T}\right)^{-1} \tag{28}$$

The thermal conductivity of the frost is calculated by using Sanders' correlation (Sanders 1974).

$$k_f = 1.202\cdot 10^{-3}\rho_f^{0.963} \tag{29}$$

2.3 The Air Side Model

2.3.1 The characteristics of mixed air

With heat recovery system, part indoor air should be mixed with outdoor air under evaporator side. Then the temperature of mixed air should be higher than that of outdoor air involved in traditional window-type air-conditioners, and which can heat the surface of the evaporator. The relative humidity should be decreased at the same time. Both would reduce the possibility of frosting. It is assumed that the outdoor fresh air and indoor air are mixed completed. Then the characteristics of the mixed air would be determined as follows:

$$\dot{m}_a = \dot{m}_{o.a} + \dot{m}_{i.a} \tag{30}$$

$$d_a = \frac{d_{o.a}\dot{m}_{o.a} + d_{i.a}\dot{m}_{i.a}}{\dot{m}_a} \tag{31}$$

Where, the term of $\frac{\dot{m}_{fr.a}}{\dot{m}_a}$ means the mass ratio of the fresh air. From the equations mentioned above, the characteristics of the mixed air, i.e. inlet air could be obtained.

2.3.2 The air side pressure drop

The airside pressure drop was evaluated based on Kays and London (1992).

$$\Delta p_a = \frac{G_{\max}^2}{2 \cdot \rho_l}\left[\left(1+\sigma^2\right)\left(\frac{\rho_i}{\rho_e} - 1\right) + f_a \cdot \frac{A_T}{A_{\min}} \cdot \frac{\rho_i}{\rho_m}\right] \tag{32}$$

Where, f_a is correlated by Karatas (1995) as,

$$f_a = 0.152 \cdot \mathrm{Re}^{-0.164}\, \varepsilon^{-0.331} \tag{33}$$

3 RESULTS AND DISCUSSION

The discussions are all based on the above characteristics of mixed air. The characteristics of mixing indoor and outdoor air are shown in the Table 1.

Table 1. Characteristics of mixing outdoor air and indoor air

	outdoor air			indoor air			mixed air	
Case 1	t	relative humidity	ratio	T	relative humidity	ratio	t	Relative humidity
	-10^{0}C	30%	80%	15^{0}C	42%	20%	-5^{0}C	50%
	-10^{0}C	30%	60%	15^{0}C	36%	40%	0^{0}C	50%
	-5^{0}C	30%	40%	20^{0}C	40%	60%	+10^{0}C	50%
Case 2	t	relative humidity	ratio	T	relative humidity	ratio	t	Relative humidity
	-15^{0}C	30%	70%	18.3^{0}C	42%	30%	-5^{0}C	50%
	-15^{0}C	30%	60%	10^{0}C	45%	40%	-5^{0}C	60%
	-15^{0}C	30%	50%	5^{0}C	62%	50%	-5^{0}C	70%

3.1 Effects of The Air Inlet Temperature

Figures. 1 (a), (b), (c) show the effects of the air inlet temperature on the total heat transfer coefficient, frost thickness and the air side pressure drop separately. In these figures, the air inlet temperature is the mixed air temperature. As can be seen from Fig. 1, higher total heat transfer will be obtained with the increased time. Furthermore, heat transfer is faster at start, and then slowly goes to the balance. The capability of heat exchange is the largest when the mixed air temperature equals –5℃, the reason of that may be that the mixed air temperature is not high enough to heat the surface of the evaporator, moreover, it is even higher than that without heat recovery system, and the environment temperature is lower than –5℃(Rite, 1990).

However, UA_T are much smaller as the mixed air temperatures are at 0℃ or 10℃. The frost thickness almost approaches to linear accumulation in Figure 2. It takes only about 3 hours for -5℃ to form 0.5mm thick frost, but for 0℃, 8 hours. The frost is almost no accumulation for air inlet temperature is equal to 10℃. It shows that there is almost no heat and mass transfer between air and cold coil surface of evaporator under this condition. It can be seen from Fig. 1 (c) that the airside pressure drop increases rapidly as air inlet temperature is -5℃, but slowly for 0℃ and 10℃. For airside pressure drop has significant influence to the formation of frost, therefore, lower pressure drops results in less frost, it also can be concluded from the Figure 1 (b).

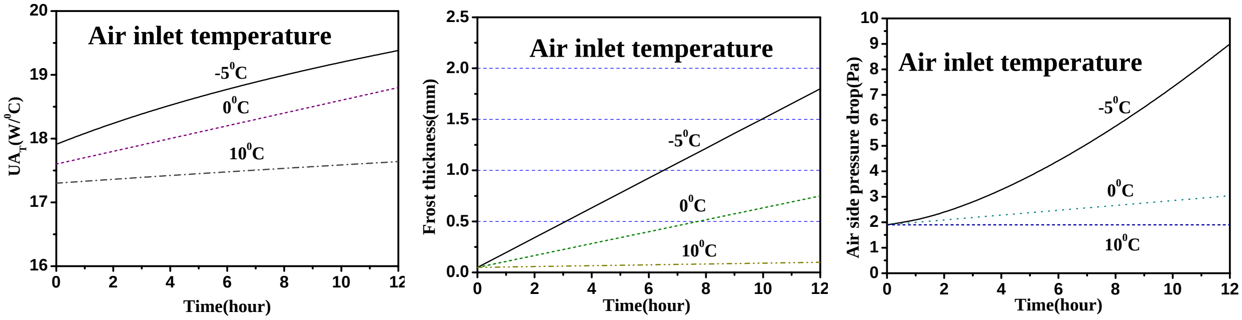

(a) on the total heat transfer coefficient **(b) Frost thickness** **(c) On air side pressure drop**

Fig. 1. Effects of the air inlet temperature
(Air mass flow: 15 l/s; Surface temperature: -15℃; -10℃ for mixed temperature=10℃;
Relative humidity: 50%; Fin pitch: 10mm)

3.2 Effects of Relative Humidity

Figures 2 (a), (b), (c) present the variances of the total heat transfer coefficient, frost thickness and airside pressure drop with relative humidities are 70%, 60% and 50% respectively. Not like the influence of the air inlet temperature, the relative humidity mostly effect the mass transfer, and at the same air inlet temperature, higher relative humidity shows the higher water vapor in the air, i.e. the greater driving potential frost accumulation and the faster the increase of frost thickness. This helps explain why the evaporator of air-source window-type air conditioner frosts severely at high ambient humidity when operated in heating mode. As shown in Figure 2 (a), increase of relative humidity increases total heat transfer coefficient, but the rate of increase slowly diminishes with time.

Increase of relative humidity also increases pressure drop and frost thickness. Since with the heat recovery system in winter, the characteristics of mixed air would change greatly sometime, for example, if outdoor air is -15°C, the relative humidity is 30%, and the fresh air ratio is 70%; the indoor air is 18.3°C, relative humidity is 42% and the ratio is 30%, the relative humidity of the mixed air is 50%, higher than that of both the outdoor air and the indoor air (Table 1). Because of the essence variance of the air characteristics, it therefore results to the heat and mass transfer process. It is noted that from Figure 2 (b) that the frost thickness increases non-linearly with frosting time, fast increase at the start and gradually slowing down afterwards. This is because the density of frost at layer close to tubes gradually increases with the time as water vapor penetrates and solidifies through these layers. Airside pressure drop increases rapidly with increasing frost thickness. This is because that the increased frost thickness leads to a narrower fin pitch and a smaller airflow passage area and, hence, the air velocity and pressure drop greatly increase. The frost accumulation and airside pressure drop have tightly contacted each other. Thus parameters in the equation of airside pressure drop also have influence to the frost formation. Such as relative humidity, the higher the mixed air relative humidity is, the more rapidly the air pressure drop increases. It can be illuminated by the fact that moisture content increases with the increases of relative humidity at a constant air temperature, and consequently, more frost is accumulated.

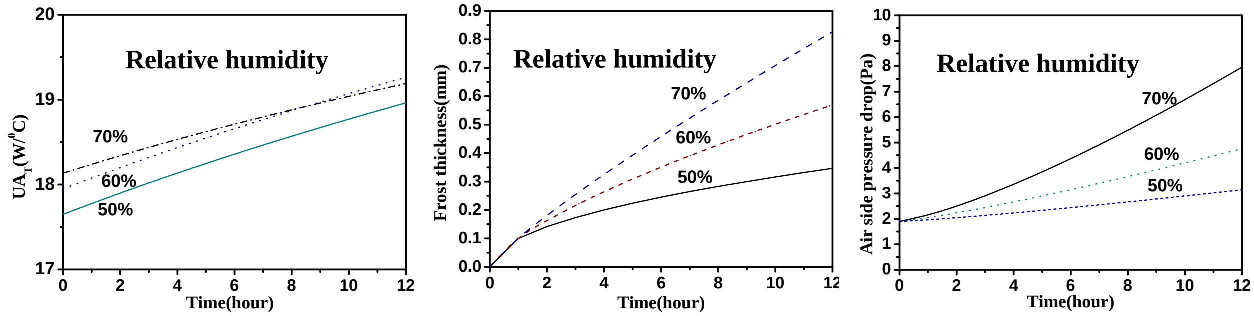

(a) on total heat transfer coefficient **(b) On frost thickness** **(c) On air side pressure drop**

Fig. 2. Effects of the relative humidity

(Inlet air temperature:5℃; Air mass flow rate:15 l/s; Surface temperature:-12℃; Fin pitch: 10 mm)

3.3 Effects of Air Mass Flow Rate

Figures 3(a), (b), and (c) indicate the effects of varying air mass flow rate on total heat transfer coefficient, frost thickness and airside pressure drop. All the figures show that increase of air mass flow rate increases total heat transfer coefficient, airside pressure drop, and frost thickness. The known air inlet temperature, relative humidity, and surface temperature are the same as the above analysis. However, the rates of total heat transfer coefficient variances are almost the same with the air mass flow rate changing, and the increase of the UA_T will therefore the same of all the three conditions with the time diminished, only the initial values are different. The more the air mass flow rate, the greater the initial UA_T is. Figure.3 (c) depicts the effects of varying air mass flow rate on frost formation. At a higher air mass flow rate, less frost could be accumulated on coil surface, because the increase of air mass flow rate, i.e. increase of air velocity, would lead to a decrease of frost surface roughness and an increase in frost density, making the penetration of water vapor into a frost layer more difficult. Therefore, for a window-type heat pump, increasing the air mass flow rate would be a method that may be considered to delay frost formation and growth. However, this could increase the resistance to airflow, and the airside pressure drop as shown in Figure 3 (c).

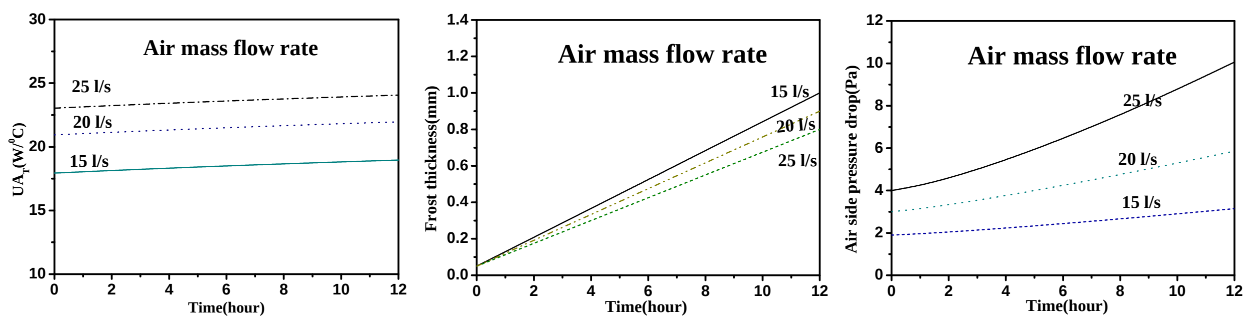

(a) On the total heat transfer coefficient **(b) On the frost thickness** **(c) On airside pressure drop**

Fig. 3. Effects of air mass flow rate

(Inlet air temperature: 5℃; Relative humidity: 50; Surface temperature: -12℃; Fin pitch: 10 mm)

4 CONCLUSIONS

A mathematic model of widow-type heat pump with heat recovery system under frosting has been developed. This model was used to calculate the unsteady thermal characteristics of fin-and-tube heat exchanger under force convection condition. With heat recovery system, temperature of mixed air , i.e. evaporator inlet air temperature would increase, but in terms of relative humidity, would do according to the relative humidity of the indoor air and outdoor air and their ratio. The model was partially based on utilizing empirical correlations for predicting frost thermal conductivity and the amount of water vapor increasing the frost density. Parameter analysis has been carried out to investigate the variance of the total heat transfer coefficient, frost thickness and airside pressure drop in terms of different air inlet temperature, relative humidity and air mass flow rate separately.

Rationalizing ratio and characteristics of indoor air and outdoor air could prolong frosting time and reduce the frost thickness greatly.

The results show that total heat transfer will increase with the time diminishes when varying air inlet temperature. Furthermore, heat transfer is faster at start, and then slowly goes to equilibrium. The same trends could be investigated for the airside pressure drop and frost thickness.The higher water vapor in the air results in the faster the increase of frost thickness and total heat transfer coefficient, but the increased rate slowly diminishes with time. Enhancement of relative humidity also increases pressure drop. The frost thickness increases non-linearly with frosting time, increases fast at the start and gradually slows down afterwards. The rates of total heat transfer coefficient variances are almost the same as the air mass flow rate changing, and the increase of the UA_T will therefore the same of all the three conditions with the diminished time, only the initial values are different. A higher air mass flow rate can accumulate less frost . However, this could increase the airflow resistance , and the airside pressure drop.

REFERENCES

Hambraeus K. 1991. “Heat transfer coefficient during two phase flow boiling of HFC-134a,” *International Journal of Refrigeration*, Vol. 14, pp. 357-362.

Jones B. W. and J. D. Parker, 1975. “Frost formation with varying environment parameters,” *Journal of Heat Transfer*, Vol. 97, pp. 255-259.

Karatas H., 1995. “Theoretically and experimentally investigation of a domestic refrigerator evaporator,” MSc Thesis, Technology University of Istanbul-Institute of Science and Technology.

Kays W. M., and A. L. London. 1992. *Compact heat exchangers*, 3rd ed. McGraw Hill, Singapore.

Kondepudi S. N., and D. L. O’Neal. 1993. “A simplified model of pin fin heat exchangers under frosting conditions,” *ASHRAE Transactions*, Vol. 99, Part 1, pp. 754-761.

Liu Z. Q., G. F. Tang, and F.Y. Zhao. 2003. “Dynamic simulation of air-source heat pump during hot-gas defrost.” Vol. 23, pp. 675-685.

Madi M. A., R. A. Johns, and M. R. Heikal. 1998. “Performance characteristics correlation for round tube and plate finned heat exchanger,” *International Journal of Refrigeration*, Vol. 21, pp. 507-517.

Marinyuk B. T. 1980. “Heat and mass transfer under frosting conditions,” *International Journal of Refrigeration*, Vol. 3, pp. 366-368.

Miller W.A. 1978. “Laboratory examination and seasonal analysis of frosting and defrosting for an air-to-air heat pump,” *ASHRAE Transactions*, Vol. 93, Part 1, pp. 1474-1489.

Neal D. L., K. T. Peterson, N. K. Anand, and J. S. Schliesing. 1989. “Refrigeration system dynamics during the reverse cycle defrost," *ASHRAE Transactions*, Vol. 95, Part 2, pp. 689-698.

Rite R. W. 1990. "The effect of frosting on the performance of domestic refrigerator-freezer finned tube evaporator coils," Master Thesis, University of Illinois, USA.

Sami S. M. and T. Duong. 1989. "Mass and heat transfer during frost growth," *ASHRAE Transactions*. Vol. 95, Part 1, pp. 158-164.

Sanders C. 1974. "The influence of frost formation and defrosting on the performance of air coolers," PhD Dissertation, Delft University，Netherlands.

Thomas H. K., J. W. Ramsey, J. L. Threlkeld. 1998. *Thermal environmental engineering*, 3rd edition, Prentice Hall.

Yonko J. D. and C.F. Sepsy. 1967. "An investigation of the thermal conductivity of frost while forming on a flat horizontal plate." *ASHRAE Transactions*, Vol. 73, Part 1, pp. 1-10.

Young D. J. 1980. "Development of a northern climate residential air-source heat pump," *ASHRAE Transactions*, Vol. 86, pp. 671-686.

Nomenclature

a	constant / coefficient	$\dot{m}$	mass flow / accumulation rate (kgs^{-1})
A	Area (m^2)	m	parameter defined by Equ.27
c_p	special heat capability (Jkg^{-1}K^{-1})	Pr	Prandtl number
c	transfer coefficient (heat/mass) (W m^{-2} K^{-1})	p	Pressure (Pa)
d	absolute humidity (kg kg^{-1}) / diameter (mm)	Q	energy (W)
D	diameter of pipe (m)	R	gas constant of water vapor
D_s	diffusivity of water vapor in air (m^{2}s^{-1})	Re	Reynolds number
f_a	fanning factor	Re_{l0}	Refrigerant Reynolds number for liquid phase
G	mass flux (kg m^2 s^{-1})	S	distance (m)
h	enthalpy (kJkg^{-1})	t	time (s)
k	Thermal conductivity (W m^{-1} K^{-1})	T	Temperature (°C)
L	fin equivalent height (m)	x	lateral coordinate (m)
Le	Lewis number		
Greek symbols			
α	Heat transfer coefficient (W m^2 K^{-1})	ρ	air density (kgm^{-3})
λ	thermal conductivity (Wm^{-1}K^{-1})	η	efficiency
δ	Thickness/height (mm)	Δ	difference
ν	kinematics viscosity (m^2 s^{-1})	σ	finning factor
Subscripts			
a/ai	air	*max*	maximum
con	conduction	*min*	minimum

e	evaporator	*o*	outdoor / outside
eff	efficient	*T / t*	total
f	fin	*v*	vapor
fr	frost	*s/sur*	surface
I	indoor / ice / inside	*sb*	Sublimation of water vapor
L	liquid	*sv*	sublimation
lat	latent	δ	thickness/height
m	mass	ρ	air density (kg m^{-3})

ACKNOWLEDGMENTS

The authors gratefully acknowledge the financial support of National Natural Science Foundation of China (No. 50408019).